electronics

MDPI

Article

High-Efficiency 5G-Band Rectifier with Impedance Dispersion Compensation Network

Yiyang Kong, Xue Bai, Leijun Xu * and Jianfeng Chen

School of Electrical and Information Engineering, Jiangsu University, Zhenjiang 212013, China; 2212207077@stmail.ujs.edu.cn (Y.K.); baixue@ujs.edu.cn (X.B.); 1000005767@ujs.edu.cn (J.C.)
* Correspondence: xlking@ujs.edu.cn

Abstract: This paper proposes a microwave rectifier designed for the popular 5G band, featuring impedance dispersion compensation and a cross-type impedance matching network. The rectifier has an ultra-high power conversion efficiency. The compensation network employs two parallel transmission lines to counteract the nonlinear shift of the diode input impedance caused by frequency variation. Additionally, the cross-over impedance matching network enhances matching and minimizes losses. After rigorous theoretical analysis and simulation, the rectifier is fabricated. Experimental results show significant conversion efficiency in the 5G band (across 4–6.5 GHz). At an input power of 12 dBm, the rectifier achieves more than 60% efficiency between 4.8 and 6.4 GHz and more than 70% between 5.2 and 6.2 GHz, with a peak efficiency of 78.1%. Moreover, the rectifier maintains more than 50% efficiency over a wide input power range of 5 to 14 dBm.

Keywords: energy harvesting; 5G rectifier; impedance dispersion compensation; high efficiency; wireless power transfer (WPT)

check for updates

Citation: Kong, Y.; Bai, X.; Xu, L.; Chen, J. High-Efficiency 5G-Band Rectifier with Impedance Dispersion Compensation Network. *Electronics* **2024**, *13*, 3105. https://doi.org/10.3390/electronics13163105

Academic Editor: Federico Moro

Received: 13 July 2024
Revised: 2 August 2024
Accepted: 5 August 2024
Published: 6 August 2024

Copyright: © 2024 by the authors. Licensee MDPI, Basel, Switzerland. This article is an open access article distributed under the terms and conditions of the Creative Commons Attribution (CC BY) license (https://creativecommons.org/licenses/by/4.0/).

1. Introduction

Wireless power transfer (WPT) technology has garnered significant attention as an innovative approach to wireless power supply, with energy harvesting (EH) playing a pivotal role in its advancement. EH systems have the capability to capture ambient electromagnetic energy from various sources, converting it into usable electrical power for wireless devices. As modern wireless communication technology progresses rapidly, 5G WIFI signals have permeated our environment and daily life, thereby extending the scope of electromagnetic energy that can be harvested by EH systems. This expansion encompasses not only traditional electromagnetic spectrums such as Digital Television (DTV), GSM900, GSM1800, 3G, and 4G but also the emerging 5G spectrum, unlocking even greater potential for EH applications [1].

Rectifiers are a crucial component within EH systems, which convert the harvested electromagnetic energy into a usable form. However, rectifier diodes exhibit nonlinear variations in input impedance depending on the operating frequency and input power level. This nonlinearity can lead to fluctuations in their performance across different environments, making it challenging to maintain consistent and efficient power conversion [2]. Impedance mismatch between the rectifier and the energy source can significantly impact the power conversion efficiency (PCE), reducing the overall effectiveness of the EH system. Ensuring high PCE across the entire 5G bandwidth spectrum represents a significant challenge for rectifiers. The wide frequency range and high data rates associated with 5G signals demand rectifiers that can efficiently handle varying input power levels and frequencies. To address this challenge, researchers are exploring various techniques to enhance the performance of rectifiers in EH systems. One approach involves the use of advanced circuit design and optimization techniques to minimize impedance mismatch and improve power conversion efficiency. By carefully selecting and configuring the components of the rectifier

circuit, it is possible to achieve better impedance matching and higher PCE across the 5G spectrum. Another approach involves the use of adaptive algorithms and control strategies to dynamically adjust the rectifier's input impedance based on the operating frequency and input power level [3,4]. These algorithms can monitor the performance of the rectifier in real-time and make adjustments to optimize its performance in different environments. By continuously adapting to changing conditions, these adaptive rectifiers can maintain high PCE across the entire 5G bandwidth spectrum, enhancing the overall efficiency and reliability of EH systems. Furthermore, advancements in semiconductor technology are enabling the development of new rectifier diode materials with improved characteristics [5]. These materials offer higher breakdown voltages, lower leakage currents, and better temperature stability, allowing for more efficient and reliable power conversion. By incorporating these advanced diode materials into EH systems, it is possible to achieve even higher PCE and enhance the overall performance of wireless power transfer technology. In addition to these technical advancements, researchers are also exploring novel EH system architectures that can better harness the vast potential of 5G signals. For example, multi-band and wideband EH systems are being developed to simultaneously capture energy from multiple frequency bands within the 5G spectrum. These systems employ advanced filtering and rectification techniques to efficiently convert the harvested energy into usable electrical power, further enhancing the overall performance and efficiency of WPT technology [6].

In recent years, most of the studies proposed impedance matching for multi-band and broadband rectifiers, and there are few studies on rectifiers operating in the 5G band [7–11]. With the advent of the 5G era, these researches give more inspiration. In previous studies, there are more rectifiers designed for a single frequency of 5.8 GHz. Defu Wang et al. realized the dual-frequency operation capability of the rectifier by using a dual-frequency matching network, and the maximum rectification efficiency can reach 51.5% at 5.8 GHz [12]. Song et al. designed a five-band rectifier consisting of two single-series diode rectifiers with an efficiency of only 38% at 5.8 GHz due to the excessive number of operating bands [13]. Jincai Qiao et al. designed a wide-input power rectifier with a maximum rectification efficiency of 64.2% at 5.8 GHz by using a dual-branch, dual-load voltage-doubling rectifier circuit structure [14]. Ahsan Halimi et al. introduced multiple transmission lines and short cutoffs in a single-band rectifier to broaden the operating band of the rectifier. The maximum PCE of this rectifier is 57.1% at 5.8 GHz. Ahsan Halimi later designed a rectifier operating in 5G and wifi bands, which utilizes a half-wavelength transmission line to broaden the second frequency band and achieves an efficiency of 45.2% at 5.8 GHz [15,16]. Yiwen Xiao designed a self-switching rectifier circuit operating at 5.8 GHz with a maximum rectification efficiency of 68.2% by connecting diodes with high and low threshold voltages in parallel [17]. Si Ce Wang et al. utilized multiple stubs to extend the input power range, which resulted in a rectifier with a rectification efficiency of up to 72% at 5.8 GHz [18]. Zeng et al. designed a C-band rectifier with harmonic suppression and ripple smoothing functional filters to achieve a peak efficiency of 74.1% at 5.8 GHz [19]. Jongseok Bae et al. designed a 5.8 GHz rectifier based on a common-ground and multi-stack structure, with a maximum conversion efficiency of 73.1% [20]. X Qin et al. proposed a rectifier design method utilizing harmonics and measured a model operating at 5.8 GHz fundamental frequency with a maximum rectification efficiency of 71.3% [21]. Z Yue et al. designed a tri-band rectifier using diode arrays with a power conversion efficiency of 73.5% at 5.8 GHz. they also designed an ultra-wideband rectifier using L-type microstrip branch and collector inductor, with a rectification efficiency of more than 60% at the 5G band [22,23]. Wu et al. used the third harmonic termination to balance the capacitive impedance of the diode at the fundamental frequency, and the proposed rectifier achieved the highest rectification efficiency of 75.6% in the 5.2–6 GHz range [24]. To extend the operating frequency to 5G, many rectifiers utilize transmission lines for input impedance matching. However, this approach often leads to an increase in overall size, which prevents maximizing the rectification efficiency.

In this paper, a novel 5G-band rectifier is introduced. This rectifier incorporates an impedance dispersion compensation circuit that includes two transmission lines linked to a diode, as well as a cross-shaped matching stub as its matching topology. Distinct from the preceding design, the presented impedance dispersion compensation circuit and matching network boast a straightforward design. This simplicity not only facilitates high RF-DC conversion efficiency within the 5G band range but also significantly diminishes the rectifier's physical dimensions.

2. Design Methodology and Simulation

Figure 1 illustrates the schematic design of the proposed rectifier that incorporates impedance dispersion compensation. This innovative design is composed of three distinct and integral components: a cross-type impedance matching network, an impedance dispersion compensated diode topology, and a load. The impedance matching network is a crucial element, consisting of three segments of microstrip lines connected in parallel with two cross-type matching stubs of the transmission line. This configuration effectively compresses the input impedance to approximately 50 Ω, ensuring optimal power transfer and minimizing reflection losses. The impedance dispersion compensation circuit is another vital part of the design, comprising two transmission lines connected in parallel. These lines are specifically engineered to be varied with frequency, allowing for precise compensation for the nonlinear impedance variation of the diode. This compensation mechanism is essential as it ensures that the diode operates efficiently across a wide range of frequencies, enhancing the overall performance and stability of the rectifier. Overall, the proposed rectifier design with impedance dispersion compensation offers a robust and efficient solution for rectifying signals while mitigating the challenges associated with impedance mismatch and nonlinear impedance variation. Its unique combination of a cross-type impedance matching network and an impedance dispersion compensated diode topology makes it a promising candidate for various applications, including wireless power transfer and energy harvesting systems.

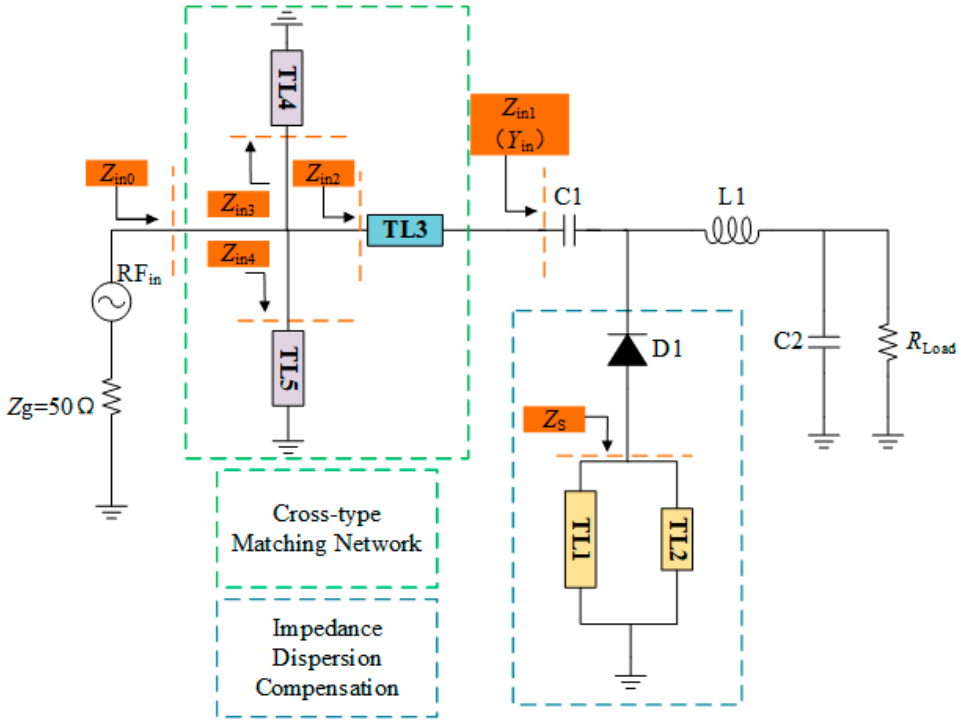


Figure 1. Schematic diagram of the proposed rectifier with impedance dispersion compensation.

Figure 2 shows a detailed circuit model of the diode, where Cj is the junction capacitance, R_j is the junction resistance, and C_p is the package capacitance [25]. Due to the

capacitive characteristics of the diode PN junction, the input impedance of the diode will change nonlinearly with frequency under high frequency conditions, so the matching process must be considered to control the change in its input impedance. To theoretically analyze the diode's input impedance, it is essential to simplify the equivalent circuit of the encapsulated diode. This simplification is achieved by representing the diode with a parallel combination of capacitance Ce and resistance Re. This simplified model facilitates a more straightforward analysis of the diode's impedance characteristics and enables engineers to design effective impedance matching networks. By utilizing this model, designers can better understand how the diode's impedance varies with frequency and can develop strategies to mitigate the impact of these variations on the overall performance of the system. Ultimately, this understanding and the ability to control the diode's input impedance are crucial for optimizing the performance of high-frequency electronic systems, such as rectifiers and wireless power transfer devices. The input impedance of a diode can be described as follows:

$$Z_D = \frac{R_e}{1 + (R_e 2\pi f C_e)^2} - j\frac{R_e^2 2\pi f C_e}{1 + (R_e 2\pi f C_e)^2} \quad (1)$$

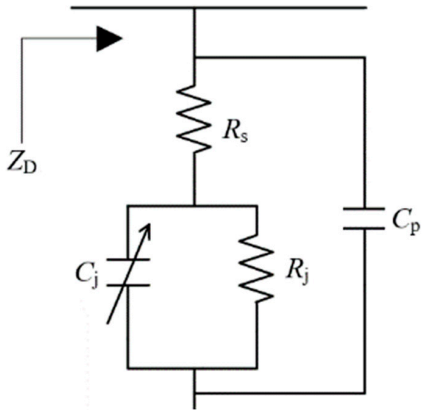


Figure 2. Diode equivalent circuit model.

As can be seen in (1), the Z_D changes with frequency f. Figure 3 shows the dispersion curves of Z_D in the 5G band for a given input power, and the trends of Real (Z_D) and Imag (Z_D) with frequency f are opposite and Imag (Z_D) changes faster. Therefore, it is necessary to balance the two changes in impedance matching.

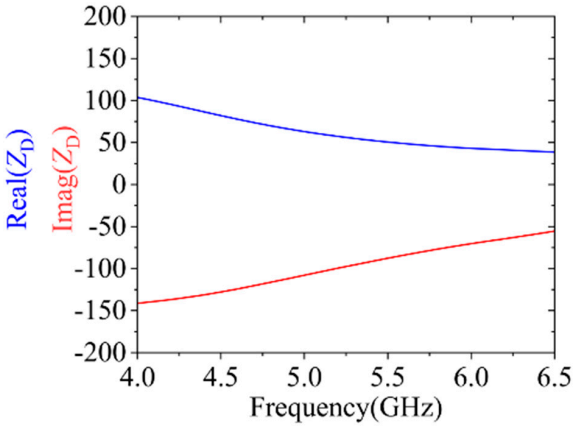


Figure 3. Dispersion curve of Z_D with frequency.

To solve this problem, an impedance dispersion compensation circuit is proposed here in series with a diode to compensate Imag (Z_D) with different amplitudes depending on

the frequency. The impedance dispersion compensation circuit consists of transmission lines TL1 and TL2 connected in parallel. Its input impedance is inductive and follows the change in frequency. Here, the center frequency of TL1 is set to be f_1 and the center frequency of TL2 is set to be f_2. The center frequencies f_1 and f_2 are the ends of the desired operating band. Z_1 is the characteristic impedance of TL1 at frequency f_1 and Z_2 is the characteristic impedance of TL2 at frequency f_2. The input impedance of the impedance dispersion compensation circuit can be expressed by (2):

$$Z_S = \frac{jz_1 tan\left(\frac{\pi}{4}\frac{f}{f_1}\right) \times jz_2 tan\left(\frac{\pi}{4}\frac{f}{f_2}\right)}{jz_1 tan\left(\frac{\pi}{4}\frac{f}{f_1}\right) + jz_2 tan\left(\frac{\pi}{4}\frac{f}{f_2}\right)} \tag{2}$$

Z_{in1} is the input impedance of the impedance dispersion compensated series diode topology, $Z_{in1} = Z_D + Z_S$, which can be expressed by (3):

$$Z_{in1} = \frac{R_e}{1 + (R_e \omega C_e)^2} - j\left(\frac{R_e^2 2\pi f C_e}{1 + (R_e 2\pi f C_e)^2} - \frac{z_1 tan\left(\frac{\pi}{4}\frac{f}{f_1}\right) \times z_2 tan\left(\frac{\pi}{4}\frac{f}{f_2}\right)}{z_1 tan\left(\frac{\pi}{4}\frac{f}{f_1}\right) + z_2 tan\left(\frac{\pi}{4}\frac{f}{f_2}\right)}\right) \tag{3}$$

In (3), it can be seen that after adding the impedance dispersion compensation circuit, Z_S compensates Imag (Z_D) so that Imag (Z_{in1}) is set to 0 for subsequent matching. Since the rectifier circuit subsequently needs to add DC filters (L1, C2), the matching of the whole circuit is not perfect, and a cross-shaped matching network consisting of transmission lines TL3, TL4 and TL5 is added next to further optimize the circuit. According to the transmission line theory, the addition of TL3 affects Z_{in1}. Similarly to the previous, TL3 varies with frequency to adjust the real and imaginary parts of Z_{in1}. The characteristic impedance of TL3 is Z_3, and its electrical length is controlled by frequency. Here, we calculate the physical length of TL3 from the operating frequencies f_1 and f_2. Figure 4 illustrates the optimization principle of the cross-matching network. The impedance dispersion compensation keeps Z_{in1} near the equal resistance circle. After adding TL3, the trace of Z_{in1} is rotated clockwise to the lower right to offset the equal reactance circle to obtain Z_{in2}. The trend of the real part of Z_{in2} is the same as that of the imaginary part. In order to adjust the rotation angle so that Z_{in2} is compressed around the center of the circle, TL4 and TL5 are used as parallel short-circuit shorting lines to rotate and compress Z_{in2} toward the center of the Smith's circle diagram to obtain Z_{in0}. The degree of rotation is controlled by the electrical lengths of TL4 and TL5. According to the transmission line theory, the parallel short-circuit truncation line can be equivalent to an inductor. Z_4 is the characteristic impedance of the transmission line TL4, Z_5 is the characteristic impedance of the transmission line TL5, and the lengths of TL4 and TL5, L4 and L5, are determined by the degree of rotation required. At this point, the input impedance of the rectifier, Z_{in0} is matched to about 50 + j * 0 Ω.

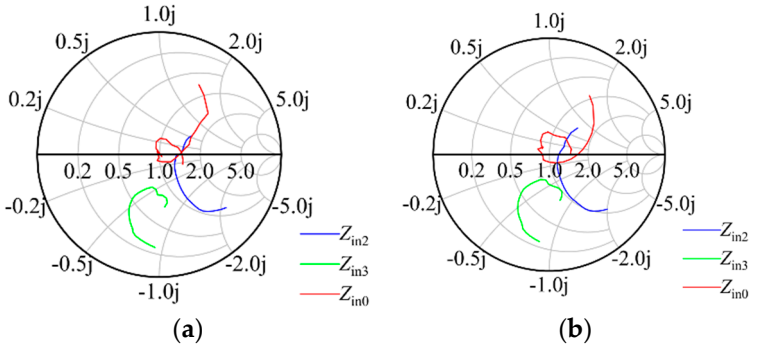


Figure 4. Impedance traces at (**a**) p = 12 dBm and (**b**) p = 9 dBm.

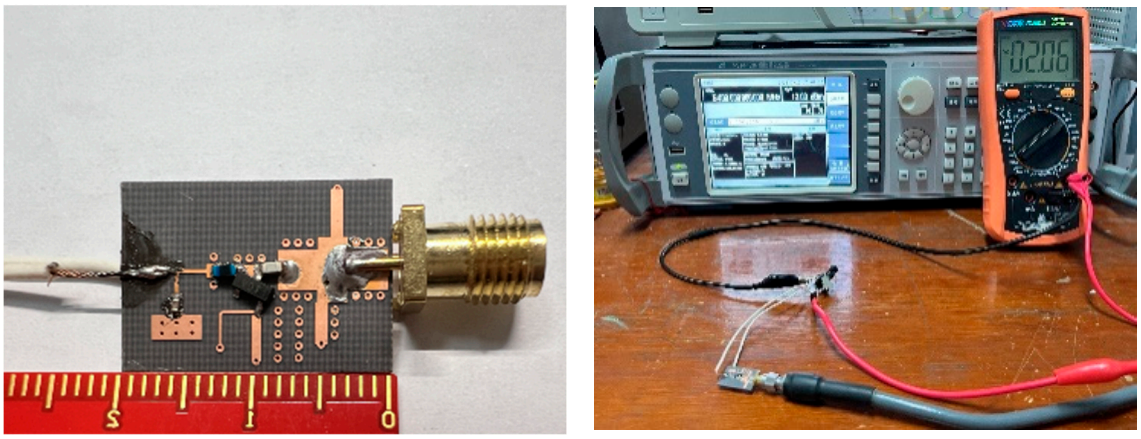
Since the rectifier needs to work in the 5G band, set f_1 to 5 GHz and f_2 to 6 GHz. The parameters of the final optimized rectifier circuit are shown in Table 1, where W1, W2, W3, W4, W5, L1, L2, L3, L4, and L5 are the lengths and widths of the transmission lines TL1, TL2, TL3, TL4, and TL5. In addition, Capacitor C1 is used for DC isolation and is 100 pF, Capacitor C2 = 100 pF, and Inductor L1 = 100 nH are Murata series.

Table 1. Size of the rectifier.

	W1/L1 (mm)	W2/L2 (mm)	W3/L3 (mm)	W4/L4 (mm)	W5/L5 (mm)
Initial	0.1/2.7	0.5/2.6	4.7/2	1.6/2.4	0.6/5.7
Optimized	0.7/3.3	0.2/2.5	2.9/2.95	0.9/3.5	0.95/3

3. Implementation and Measurement

To verify the feasibility of the design, a 1 mm thick F4B (εr = 2.65) dielectric substrate was used and the HSMS-2862 Schottky diode was selected as the rectifier diode and the photograph of the rectifier is shown in Figure 5a. The use of the HSMS-2862 diode is another significant advantage of the proposed rectifier. This diode is known for its high efficiency and reliability, making it an ideal choice for use in high-frequency electronic systems. The HSMS-2862 diode's low junction capacitance and high breakdown voltage contribute to the overall performance of the proposed rectifier, enabling it to achieve high PCE and stable operation across a wide range of input powers and frequencies. The rectifier is designed and fabricated, the layout and the photographs are shown in Figure 5a. The physical dimensions of the rectifier are 21 × 13.8 mm^2. Figure 5b shows the entire test rig. The RF signal is generated by an RF signal generator (AV1442). The load is a sliding varistor soldered directly to the rectifier. A digital multimeter is used to measure the output voltage of the load.



(**a**) (**b**)

Figure 5. (**a**) Proposed fabricated rectifier. (**b**) Photograph of the measuring setup.

The RF-to-DC conversion efficiency is defined as the ratio of the DC output power to the microwave incident power, which is calculated by the following formula:

$$\eta = \frac{V_{out}^2}{P_{in} \times R_L} \times 100\% \quad (4)$$

where V_{out} is the output voltage, P_{in} is the input power and R_L is the load resistance.

The RF source is set to 12 dBm, 9 dBm, and 6 dBm. Figure 6a–c show the simulated and actual measured S11 parameters, as well as the RF-DC power conversion efficiency and output voltages at a termination load of 450 Ω. Circuit stencil process is the main reason for some deviation in test and simulation. As shown in the figure above, the RF-DC

conversion efficiencies for 5.2–6.2 GHz are all greater than 70% when the input power is 12 dBm. The maximum RF-DC conversion efficiency of the rectifier reaches 78.1% under this power condition.

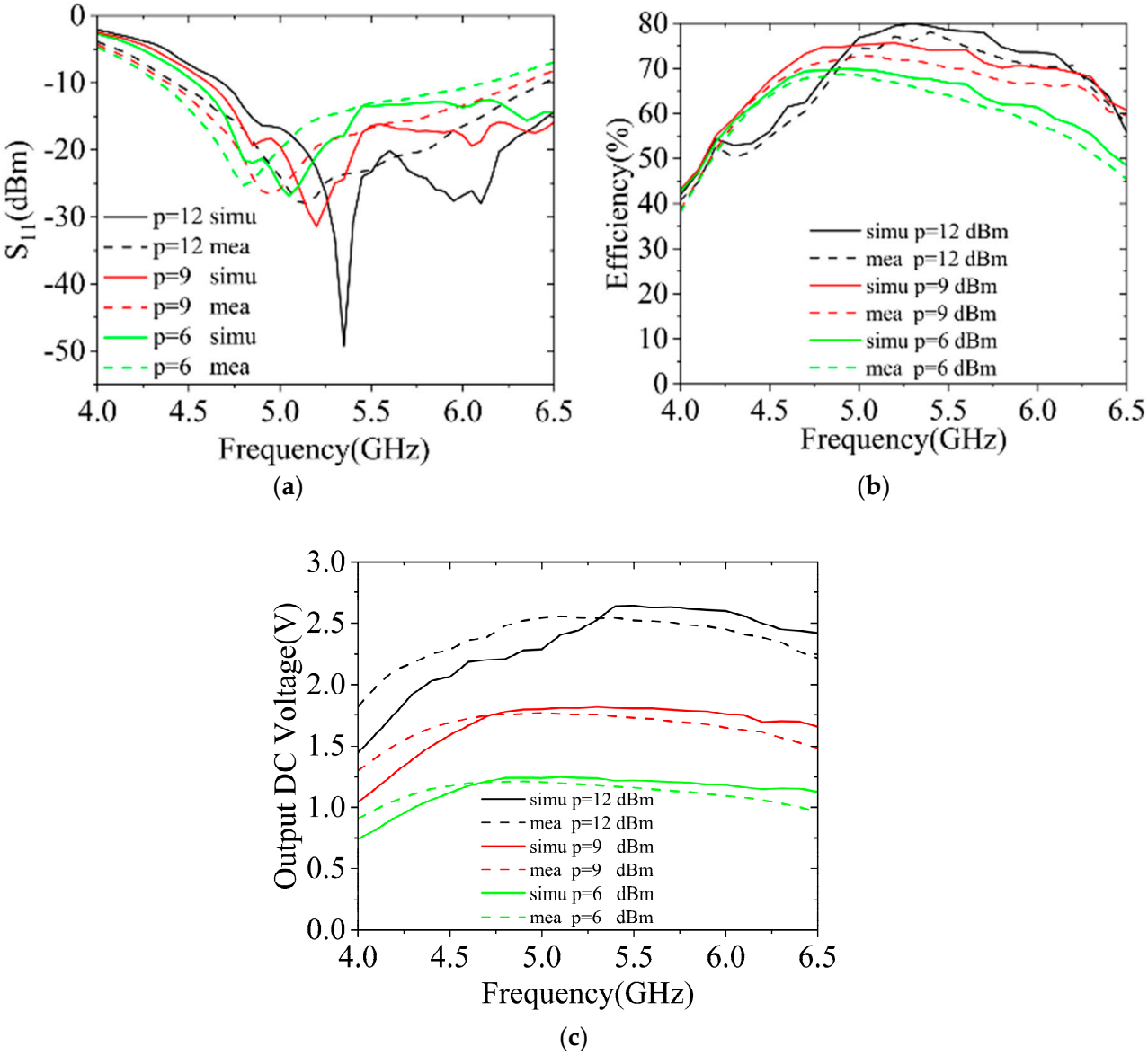


Figure 6. (**a**) Measured and simulated S11 of the rectifier for three power levels. (**b**) Measured and simulated RF-DC conversion efficiency versus frequency at three power levels. (**c**) Measured and simulated output voltage versus frequency at three power levels.

Based on the test in Figure 6, two additional test powers of 3 dBm and 0 dBm are added to conduct experiments on it and test the conversion efficiency and output voltage of the rectifier at three different frequency points. Figure 7a shows the efficiency curves obtained at various input powers. Notably, at 0 dBm input power and a 450 Ω load, the peak conversion efficiency attains 55%. Meanwhile, Figure 7b shows how energy conversion efficiency and output voltage change with varying input powers across three distinct 5G band frequencies. Remarkably, the conversion efficiency maintains over 50% for input powers between 5–14 dBm. Furthermore, Table 2 compares the performance of our proposed rectifier with existing 5G band rectifiers, highlighting its competitiveness and advancements.

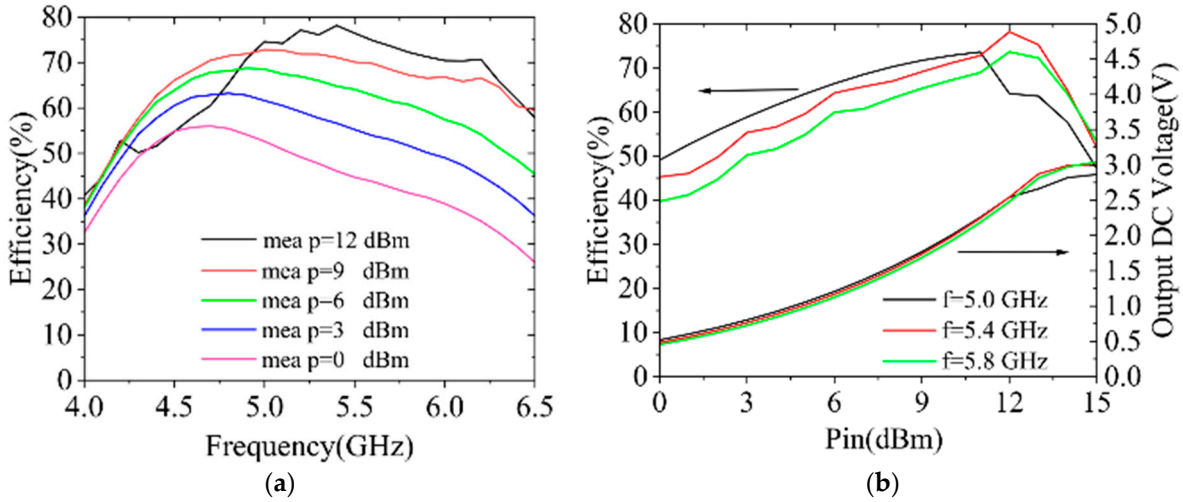


Figure 7. (**a**) Efficiency variation curve measured at five different power levels. (**b**) Measured power conversion efficiency and output DC voltage of the rectifier circuit versus input power at different frequencies with load of 450 Ω.

Table 2. Comparison with the prior rectifiers.

Ref.	Frequency (GHz)	Pin (dBm)	Max PCE	FBW of PCE > 70%	Diode Type	Size (mm^2)
[15]	5.8	0	48.9%	0	HSMS-2860	36 × 22
[16]	5.8	6.5	45.2%	0	HSMS-2860	20 × 25
[17]	5.8	28	68.2%	0	HSMS-2820	49.2 × 26.3
[18]	5.8	8–15	72%	0	HSMS-286X	/
[19]	5.8	23	74.1%	5.4–5.9 GHz	HSMS-282B	28 × 15
[20]	5.8	27	73.1%	0	MA4E1319-1	24 × 123
[21]	5.8	18.3	71.3%	0	MA4E1317	50 × 25
[22]	5.8	19	73.5%	0	MA4E1317	29.5 × 21.3
[23]	5.8	22	63%	0	MA4E1317	14.3 × 7.4
This work	5.4	12	78.1%	5.2–6.2 GHz	HSMS-2862	20 × 13.8

Table 2 presents a comprehensive comparison of the proposed rectifier with prior designs, highlighting its superior performance in several key aspects. The proposed rectifier operates at a frequency of 5.4 GHz with an input power of 12 dBm, achieving a maximum power conversion efficiency (PCE) of 78.1%. This is notably higher than several prior designs, which typically achieve maximum PCEs in the range of 50% to 75%. The higher PCE of the proposed rectifier indicates its ability to convert a larger portion of the input power into useful DC output power, making it more efficient and effective in power transfer applications. Moreover, the proposed rectifier maintains a PCE above 70% within a frequency bandwidth (FBW) of 5.2–6.2 GHz. This wide FBW indicates the rectifier's superior performance and stability across a wide frequency range. Prior designs often suffer from a narrow FBW, which limits their applicability in systems that require operation across a wide range of frequencies. The proposed rectifier's wide FBW makes it more versatile and suitable for use in various high-frequency electronic systems, such as wireless power transfer and microwave energy harvesting.

In addition to its high PCE and wide FBW, the proposed rectifier also exhibits a smaller size compared to prior designs. With dimensions of 20 × 13.8 mm^2, the proposed rectifier is more compact and suitable for use in integrated systems where space is limited.

This smaller size is achieved through the use of advanced circuit design techniques and the selection of appropriate components, such as the HSMS-2862 diode. Furthermore, the proposed rectifier's design incorporates several innovative features that enhance its performance and reliability. For example, the use of a matching network between the diode and the output filter helps to improve impedance matching and reduce power loss. The proposed rectifier's circuit design incorporates protective measures to prevent damage from high input powers or voltage spikes, ensuring reliable operation even in harsh environments.

Overall, the proposed rectifier's superior performance, wide FBW, small size, and use of high-quality components make it a promising candidate for use in various high-frequency electronic systems. Its high PCE and stable operation across a wide range of input powers and frequencies make it particularly suitable for wireless power transfer applications, where efficient and reliable power transfer is crucial. Additionally, its small size and compact design make it an ideal choice for integrated systems where space is limited.

4. Conclusions

The rectifier is suitable for the 5G band and features a simpler circuit structure than existing designs, the highest PCE at the same power, and a smaller footprint. It incorporates impedance dispersion compensation in the single diode structure to address nonlinear impedance variation with frequency. The matching network uses three transmission lines for optimal diode impedance matching and loss minimization. Rectification efficiency exceeds 70% in the 5.2–6.2 GHz range, with a peak of 78.1% at 12 dBm input power. In addition, the proposed impedance dispersion compensation structure is not complicated and can also be used for voltage-doubling structures, increasing the choice of impedance matching. This versatility makes the proposed rectifier a highly adaptable and flexible solution for various electronic systems.

Author Contributions: Writing—original draft, Writing—review & editing, Investigation, Data curation, Y.K.; Methodology, X.B.; Supervision, L.X.; Validation, J.C. All authors have read and agreed to the published version of the manuscript.

Funding: This research received no external funding.

Data Availability Statement: The raw data supporting the conclusions of this article will be made available by the authors on request.

Conflicts of Interest: The authors declare no conflict of interest.

References

1. Piñuela, M.; Mitcheson, P.D.; Lucyszyn, S. Ambient RF Energy Harvesting in Urban and Semi-Urban Environments. *IEEE Trans. Microw. Theory Tech.* **2013**, *61*, 2715–2726. [CrossRef]
2. Milosevic, B.; Radovanovic, M.; Jokanovic, B. Measurement of rectifying diode impedance and efficiency for energy harvesting applications. In Proceedings of the IEEE EUROCON 2019-18th International Conference on Smart Technologies, Novi Sad, Serbia, 1–4 July 2019; pp. 1–5.
3. Lin, H.; Chen, X.; He, Z.; Xiao, Y.; Che, W.; Liu, C. Wide Input Power Range X-Band Rectifier with Dynamic Capacitive Self-Compensation. *IEEE Microw. Wirel. Compon. Lett.* **2021**, *31*, 525–528. [CrossRef]
4. Prasanna, A.S.; Natarajamani, S. Design of Single-Band Rectifier with Self-Tuning Impedance Matching Circuit. In Proceedings of the 2020 Third International Conference on Smart Systems and Inventive Technology (ICSSIT), Tirunelveli, India, 20–22 August 2020; pp. 460–463.
5. He, Z.; Zhang, X.; Yan, L.; Che, W.; Liu, C. Analysis of Low-Power Rectifiers Based on Tunnel Diode for Energy Harvesting. In Proceedings of the 2023 16th UK-Europe-China Workshop on Millimetre Waves and Terahertz Technologies (UCMMT), Guangzhou, China, 31 August–3 September 2023; pp. 1–3.
6. Shafiq, R.R.G.; ElHalawany, B.M.; Elsherbini, M.M. Radio-Frequency Energy Harvesting Systems for GSM and WiFi Bands. In Proceedings of the 2022 IEEE International Conference on Design & Test of Integrated Micro & Nano-Systems (DTS), Cairo, Egypt, 6–9 June 2022; pp. 1–6.
7. Li, S.; Cheng, F.; Gu, C.; Yu, S.; Huang, K. Efficient Dual-Band Rectifier Using Stepped Impedance Stub Matching Network for Wireless Energy Harvesting. *IEEE Microw. Wirel. Compon. Lett.* **2021**, *31*, 921–924. [CrossRef]

8. Yu, S.; Cheng, F.; Gu, C.; Wang, C.; Huang, K. Compact and Efficient Broadband Rectifier Using T-type Matching Network. *IEEE Microw. Wirel. Compon. Lett.* **2022**, *32*, 587–590. [CrossRef]
9. He, H.; Lin, H.; Wu, P.; Li, Q.; Liu, C. Compact High-Efficiency Broadband Rectifier Based on Coupled Transmission Line. *IEEE Trans. Circuits Syst. II Express Briefs* **2022**, *69*, 4404–4408. [CrossRef]
10. Liu, W.; Huang, K.; Wang, T.; Hou, J.; Zhang, Z. A Compact High-Efficiency RF Rectifier with Widen Bandwidth. *IEEE Microw. Wirel. Compon. Lett.* **2022**, *32*, 84–87. [CrossRef]
11. Liu, W.; Huang, K.; Wang, T.; Zhang, Z.; Hou, J. A Broadband High-Efficiency RF Rectifier for Ambient RF Energy Harvesting. *IEEE Microw. Wirel. Compon. Lett.* **2020**, *30*, 1185–1188. [CrossRef]
12. Wang, D.; Negra, R. Design of a dual-band rectifier for wireless power transmission. In Proceedings of the 2013 IEEE Wireless Power Transfer (WPT), Perugia, Italy, 17–21 March 2013; pp. 127–130.
13. Song, Y.; Huang, C.; Wang, Z.; Zhang, J. Modeling of Five-Band High efficiency Rectifier for RF Energy Acquisition. In Proceedings of the 2022 11th International Conference of Information and Communication Technology (ICTech), Wuhan, China, 4–6 February 2022; pp. 498–502.
14. Qiao, J.; Zhang, B.; Niu, Z. Ultra-wide Power Range RF Rectifier Based on 5.8 GHz. In Proceedings of the 2023 16th UK-Europe-China Workshop on Millimetre Waves and Terahertz Technologies (UCMMT), Guangzhou, China, 31 August–3 September 2023; pp. 1–3.
15. Halimi, M.A.; Surender, D.; Khan, T.; Kishk, A.A.; Rengarajan, S.R. A Multistepped Transmission Line Matching Strategy Based Triple-Band Rectifier for RFEH/WPT Applications. *IEEE Microw. Wirel. Compon. Lett.* **2022**, *32*, 1007–1010. [CrossRef]
16. Halimi, M.A.; Khan, T.; Koul, S.K.; Rengarajan, S.R. A Dual-Band Rectifier Using Half-Wave Transmission Line Matching for 5G and Wi-Fi Bands RFEH/MPT Applications. *IEEE Microw. Wirel. Technol. Lett.* **2023**, *33*, 74–77. [CrossRef]
17. Xiao, Y.; Jin, K.; Zhu, X. Design of a Self-Switching Rectifier Circuit for Microwave Power Transmission. In Proceedings of the 2021 IEEE Applied Power Electronics Conference and Exposition (APEC), Phoenix, AZ, USA, 14–17 June 2021; pp. 2556–2559.
18. Wang, S.C.; Li, M.J.; Tong, M.S. A High-Efficiency Rectifier with Widening Input Power Range Based on Microwave Power Transmission. In Proceedings of the 2020 IEEE International Conference on Computational Electromagnetics (ICCEM), Singapore, 24–26 August 2020; pp. 268–269.
19. Zeng, H.; Tang, Y.; Liu, Y. Compact high-efficiency c-band rectifier with high input power for microwave power transmission. *Electron. Lett.* **2023**, *59*, e12776. [CrossRef]
20. Bae, J.; Yi, S.-H.; Choi, W.; Koo, H.; Hwang, K.C.; Lee, K.-Y.; Yang, Y. 5.8 GHz High-Efficiency RF–DC Converter Based on Common-Ground Multiple-Stack Structure. *Sensors* **2019**, *19*, 3257. [CrossRef] [PubMed]
21. Qin, X.; He, G.; Yang, X.; Gao, S. A Compact Rectifier Design Method Utilizing Harmonics. *Appl. Sci.* **2021**, *11*, 2295. [CrossRef]
22. Yue, Z.; Xu, X.; Li, S.; Zhu, Y.H.; Lin, X.Q. Efficient and Compact Tri-Band Rectifier with Large Frequency Ratio for WPT. *IEEE Microw. Wirel. Compon. Lett.* **2022**, *32*, 1355–1358. [CrossRef]
23. Yue, Z.; Xu, X.; Li, S.; Lin, X.Q.; Zhong, L.J.; Shi, M.D. Design of Efficient and Compact Ultrawideband Rectifier for Sub-6 GHz WPT/EH. *IEEE Microw. Wirel. Technol. Lett.* **2023**, *33*, 1490–1493. [CrossRef]
24. Wu, P.; Zhang, L.; Liu, C.; Zhao, Y. A C-band microwave rectifier based on harmonic termination and with input filter removed. In Proceedings of the 2017 IEEE Wireless Power Transfer Conference (WPTC), Taipei, Taiwan, 10–12 May 2017; pp. 1–4.
25. Wu, P.; Huang, S.Y.; Zhou, W.; Ren, Z.H.; Liu, Z.; Huang, K.; Liu, C. High-Efficient Rectifier with Extended Input Power Range Based on Self-Tuning Impedance Matching. *IEEE Microw. Wirel. Compon. Lett.* **2018**, *28*, 1116–1118. [CrossRef]

Disclaimer/Publisher's Note: The statements, opinions and data contained in all publications are solely those of the individual author(s) and contributor(s) and not of MDPI and/or the editor(s). MDPI and/or the editor(s) disclaim responsibility for any injury to people or property resulting from any ideas, methods, instructions or products referred to in the content.